Local structure of $[(GeTe)_2/(Sb_2Te_3)_m]_n$ super-lattices by X-ray Absorption Spectroscopy

F. d'Acapito[1], P. Kowalczyk[2], J.-Y. Raty[2, 3], C. Sabbione[2], F. Hippert[4] and P. Noé[2]

[1] CNR-IOM-OGG c/o ESRF – The European Synchrotron, F-38043 Grenoble, France.
[2] Univ. Grenoble Alpes, CEA, LETI, F-38000 Grenoble, France.
[3] CESAM-SPIN, Université de Liège and FRS-FNRS, B4000 Sart-Tilman, Belgium.
[4] Univ. Grenoble Alpes, CNRS, Grenoble INP, LMGP, F-38000 Grenoble, France.

E-mail: dacapito@esrf.fr ; pierre.noe@cea.fr

Received xxxxxx
Accepted for publication xxxxxx
Published xxxxxx

Abstract

Herein, the local structure of $[(GeTe)_2/(Sb_2Te_3)_m]_n$ chalcogenide super-lattices (SLs), which are at the basis of emerging interfacial Phase-Change Memory (iPCM), is studied by X-ray Absorption Spectroscopy (XAS) at the Ge-K edge. The quantitative analysis of the first coordination shells reveal that the SLs appear to possess a structure very similar to that of thin film of the canonical $Ge_2Sb_2Te_5$ (GST225) phase-change alloy. By comparing experimental data with *ab initio* Molecular Dynamics simulations of the EXAFS spectra, we show that chemical disorder is mandatory in order to reproduce the experimental data in the full spectral range. As a result, we can unambiguously conclude that Ge/Sb intermixing resulting from inter-diffusion of the GeTe and Sb_2Te_3 layers within SLs is inherent to SLs and is not induced by sample preparation method nor by interaction with the electron beam of electron microscopes used in all the previous studies that were suggesting such a phenomenon. We further evidence that the short Ge-Te distance is the same in GeTe and GST225 films, as well as in SLs. The main difference is the impact of disorder in GST225 and SLs. Intermixing being definitively present in $[(GeTe)_2/(Sb_2Te_3)_m]_n$ SLs, this parameter must be considered in future models aiming at going further in the understanding and the development of iPCM technology. This seems mandatory in order to allow such technology to emerge in the near future on the non-volatile memory market.

Keywords: GeTe, Sb_2Te_3, chalcogenide, interfacial phase-change memory, super-lattice, XAS, EXAFS

1. Introduction

Chalcogenide phase-change materials (PCM) are used for rewritable optical and resistive memory applications [1]. Ge-Sb-Te alloys, such as $Ge_2Sb_2Te_5$, are considered as prototypical compounds for such applications based on the reversible transition between the amorphous and crystalline phase of the PCM. The resistivity and optical reflectivity of the two phases are very different. It has recently been proposed that this very large contrast in the properties of chalcogenide PCM alloys results from a specific bonding mechanism, called "metavalent bonding", in the crystalline phase [2, 3]. Another type of phase-change memory using $GeTe/Sb_2Te_3$ super-lattices (SL) has been proposed [4]. A SL is obtained by depositing alternatively GeTe blocks (consisting typically of 2 Ge and two Te atomic planes) and a variable number of Sb_2Te_3 blocks. Thanks to so-called van der Waals epitaxy, the atomic planes of the SL are parallel to the substrate surface. Memories using these crystalline SLs exhibit significantly improved performances with respect to memories using a PCM alloy, such as lower programming current, better endurance and higher speed [4]. These improved properties were first attributed to a reversible change in the position of Ge atoms induced by the application of electrical pulses [5]. This change would lead to two crystalline states of the SL with very different electronic density of states and thus different transport properties. Since

this change occurs at the interface between GeTe and Sb_2Te_3 blocks, a memory device using these SLs was called interface Phase-Change Memory (iPCM). It has been argued that avoiding the melting process, which is necessary in the case of a PCM alloy, reduces the entropy loss and thus the energy required to achieve a high resistance state [6]. SLs were theoretically investigated by *ab initio* molecular dynamics simulations (AIMD) by Tominaga *et al* [5] who identified a number of possible structures (called *Ferro*, *Petrov*, *Inverted Petrov* and *Kooi*) differing by the stacking sequence of Ge, Sb and Te atomic planes. Considering formation energies, it was suggested that the SL should consist in a mixture of *Ferro* and *Kooi* structures. All these model structures contain only pure Ge, Sb and Te atomic planes.

However, further studies of GeTe/Sb_2Te_3 SLs have revealed that the deposited material differs significantly from the above models. X-ray Absorption Spectroscopy and Transmission Electron Microscopy (TEM) studies on SLs grown by Molecular Beam Epitaxy (MBE) showed the presence of intermixing between Ge and Sb as well as the absence of GeTe blocks in a [GeTe (1 nm)/Sb_2Te_3 (3 nm)]$_{15}$ SL [7, 8]. These observations were later confirmed on SLs grown by Pulsed Laser Deposition (PLD) [9]. A stacking of Sb_2Te_3 blocks (5 atomic planes) and different Ge-Sb-Te blocks (containing either 7, 9 or 11 atomic planes) separated by van der Waals (vdW) gaps is observed in TEM images [9]. In the Ge-Sb-Te blocks, pure Te planes alternate with planes occupied by a mixture of Ge and Sb. These Ge-Sb-Te blocks are similar to those found in the stable rhombohedral $(GeTe)_{m(}Sb_2Te_3)_n$ alloys.

However, these results were obtained on SLs deposited by MBE and PLD whereas iPCM devices use SLs deposited by magnetron sputtering. Since the SL structure can depend on the deposition parameters and methods, it was necessary to also study SLs deposited by sputtering [10, 11]. By means of advanced Scanning Transmission Electron Microscopy (STEM) on state-of-the-art high quality stoichiometric SLs grown by industrial magnetron sputtering, we have shown that no GeTe layer subsists and that Ge atoms intermix with Sb atoms in, for instance, $Ge_2Sb_2Te_5$ blocks, although the overall stoichiometry is that of an ideal SL [11]. Therefore, an alternative model to the ones initially proposed [6] is needed to explain the origin of the electrical contrast and the nature of the resistive switching in iPCM devices. However, the preparation of the TEM foil or possible electron beam induced damages during the acquisition of the TEM images could have affected the interface between GeTe/Sb_2Te_3 layers and locally induced a Ge/Sb intermixing. It has been shown that the stacking of the atomic planes can be reconfigured under electron irradiation [12, 13]. Therefore, a method that does not require any sample preparation is required in order to be able to draw definitive conclusions on the local structure of SLs. This is the case of X-ray Absorption Spectroscopy (XAS). Room-temperature X-ray absorption near edge structure (XANES) at the Ge K-edge has been recently investigated in sputtered SL films with various thickness of the Sb_2Te_3 layer [14]. The aim of the present work was to investigate directly the local structure around Ge atoms by analyzing the EXAFS oscillations at the Ge K-edge and hence getting information on interatomic distances between Ge atoms and their neighbors and on the nature and number of neighbors in prototypical GeTe/Sb_2Te_3 SLs grown by magnetron sputtering.

Herein, the local structure around Ge atoms by means of XAS at the Ge K-edge in prototypical GeTe/Sb_2Te_3 SLs grown by magnetron sputtering. SLs with Sb_2Te_3 layer thickness varying from 1 to 8 nm have been studied. In particular, it was necessary to probe the local order around Ge atoms in Sb_2Te_3-rich SLs, for which the best performance of iPCM devices has been reported [6, 15]. Contrary to previous XAS studies performed at room temperature [8, 14], the present XAS experiment has been performed at ≈120 K, which leads to an increase of the EXAFS signal by reducing the influence of thermal vibrations.

2. Experimental Details

2.1 Sample preparation

$[(GeTe)_2/(Sb_2Te_3)_m]_n$ SLs were deposited at 250°C on 200 mm diameter (100) silicon substrates by means of magnetron sputtering in an ultra-high vacuum industrial deposition cluster tool. Details on SL's growth can be found in reference [11]. A 5 nm thick Sb_2Te_3 buffer layer was first deposited on the Si substrate in order to allow the growth of a highly-oriented SL with atomic planes parallel to the substrate. The GeTe layer thickness was fixed to 0.7 nm, which corresponds to a single $(GeTe)_2$ block (2 Ge and 2 Te planes) in the rhombohedral GeTe crystalline phase [16]. The thickness of the Sb_2Te_3 layer is determined by m, the number of 1 nm-thick quintuple (QL) Sb_2Te_3 blocks [17].

A first series of three $[(GeTe)_2/(Sb_2Te_3)_m]_n$ SLs of 24 periods (n=24) was deposited with m = 1, 4 or 8, corresponding to a Sb_2Te_3 layer thickness equal to 1, 4 or 8 nm. These SLs were obtained by alternatively sputtering pure GeTe and Sb_2Te_3 targets. A second series of three $[(GeTe)_2/(Sb_2Te_3)_m]_{24}$ SLs with m = 1, 2 or 4 was also deposited. In the latter case, the deposition of the Sb_2Te_3 layers was made by co-sputtering of the Sb_2Te_3 target and an additional pure Te target (with 20W applied to the Te target). This method avoids a Te deficiency in the deposited SL and hence allows to get the expected stoichiometry [11]. The composition of all these SLs has been measured by Wavelength Dispersive X-Ray Fluorescence (WDXRF) and their structure and crystalline orientation have been investigated in details by X-ray Diffraction in reference [11]. The origin of the beneficial effect of Te co-sputtering on

both crystalline orientation and composition of the SLs is now unveiled in a very recent paper also published in the current Special Issue on PCM [18]. This results from the Te atomic layer forming at the substrate's growth surface compensating any possible loss of Te even also during GeTe layer growth as confirmed by SLs' composition analysis in reference [11]. For purpose of comparison, we also studied crystalline $Ge_2Sb_2Te_5$ (GST225) and GeTe thin films deposited by using the same sputtering equipment.

A 100 nm thick film of crystalline GST225 was deposited at 250°C by sputtering of a target with the same composition. Deposition at 250°C ensures a crystalline orientation of the Ge/Sb and Te planes of the rhombohedral $Ge_2Sb_2Te_5$ phase [19, 20] similar to that in the SLs, *i.e.* the atomic planes are parallel to the substrate. One part of this GST225 film was then annealed for 15 min at 400°C in a pure N_2 atmosphere. For sake of comparison, we also deposited a GST225 film in the same sputtering conditions but at room temperature. This initially amorphous film (500 nm thick) was then annealed for 40 min at 400°C in a pure N_2 atmosphere in order to crystallize it into the GST225 rhombohedral phase. This film contains crystallites with all possible orientations although a small texture may be present.

A 100 nm thick GeTe film was deposited by sputtering of a single GeTe target at 250°C. As in the case of GST225, deposition at 250°C ensures a crystalline orientation of the Ge and Te planes of the rhombohedral GeTe phase parallel to the substrate. This film proved to be slightly deficient in Te, its composition determined by WDXRF being $Ge_{51.9}Te_{48.1}$. Since the rhombohedral GeTe phase only exists in a narrow composition range [21], an excess of Ge leads to the formation of a foreign pure Ge phase (crystalline or amorphous according to the maximum temperature reached by the film [22]) in addition to the rhombohedral GeTe phase. The contribution of this Ge phase to the EXAFS signal measured at the Ge K-edge is significant (see **Figure S1** in the supplementary material). In order to suppress it, we have deposited another GeTe film at 250°C by co-sputtering of the GeTe target and a pure Te target (with 20 W applied to the Te target). The power applied to the Te target was not optimized and the composition of this film is $Ge_{42.2}Te_{57.8}$. It contains a pure Te phase in addition to the rhombohedral GeTe phase. The presence of a Te phase has no impact on the structure of the GeTe phase. As shown below, the EXAFS spectrum of that sample at the Ge K-edge is in perfect agreement with the spectrum expected for the GeTe rhombohedral structure [23]. Note that all SLs and thin films were capped *in situ* by a 10 nm thick SiN_x layer in order to protect them from oxidation after fabrication.

2.2 X-ray Absorption Spectroscopy experiment

2.2.1 Data collection of Extended X-ray Absorption Fine Structure (EXAFS) from XAS experiment

EXAFS spectra at the Ge-K edge (E=11103 eV) were collected at the LISA beamline at the ESRF (in the beamline configuration detailed in reference [24]). The monochromator was equipped with a pair of Si(311) crystals and operated in dynamically focusing mode. Two Pd coated mirrors with cut-off energy E_{cutoff} =18 keV were used for vertical focusing and harmonic rejection. Data collection was carried out in fluorescence mode using a hyper-pure Ge detector array (12 elements). Samples were positioned in grazing incidence, with an angle of 1-2° with respect to the impinging beam, by using a manipulator developed *ad hoc* for this data collection method [25]. Samples were cooled with liquid nitrogen to a temperature ≈120 K. Two to four spectra per sample were averaged to reduce the noise.

2.2.2 EXAFS data modelling

EXAFS data were extracted and fitted with the ATHENA and ARTEMIS codes and the theoretical paths for the quantitative data analysis were calculated with the Feff8.4 code [26]. Quantitative fits were carried out in R space with a total amplitude calibration factor S_0^2=0.9 derived from the fit of a crystalline Ge sample. For the *ab initio* calculation of the XAS signals, the scattering potentials were calculated starting from a Self-Consistent Field method for the electron densities plus a Hedin-Lundquist approximation for the exchange-correlation part. For all samples, we fitted the data (group at 1.9-3.6 Å in the FT) with two Ge-Te contributions (two shell model) using the theoretical paths at 2.97 and 3.05 Å. The shell radius R and a Debye Waller factor σ^2 for each shell were used as free fit parameters. The number of Te in each shell (N) was set at 3. In the case of GeTe, we also modelled the EXAFS spectra in the full R range including paths up to a total length of calculated from the structure determined by diffraction [23]. The fit parameters were the same as above for the first two shells and then the rest of the structure was fitted adjusting by scaling the cell dimensions and using a Debye model for the σ^2 factors as implemented in the Feffit code**.**

2.3 Ab Initio Molecular Dynamics (AIMD) simulation of the EXAFS spectra

Ab initio calculations of the EXAFS spectra were carried out in the framework of Density Functional Theory using the VASP [27] code. For the reference GeTe and GST225 alloys, we started from the lattice parameters and atomic positions given in references [23] and [19] and first carried out a DFT structural relaxation in order to minimize the energy. Calculations were done with projector augmented wave (PAW) pseudopotentials and the exchange-correlation functional used was the Perdew-Burke-Ernzerhof for solids

(PBEsol) [28]. At each ionic step, the electronic structure has been optimized until attaining a convergence of the total energy within 10^{-6} eV, whereas the atomic positions were optimized until Hellman-Feynman forces were below 10^{-4} eV/Å. For energy minimization, the rhombohedral GeTe phase was described by using a hexagonal unit cell containing 3 Ge and 3 Te atoms. In the case of the rhombohedral GST225 phase, the usual hexagonal unit cell (containing 9 atoms) could not be used because there are atomic sites with a mixed Ge/Sb occupation. Then a larger hexagonal cell (containing 81 atoms) was created by combining 3×3×1 hexagonal unit cells. The Ge/Sb sites in this unit cell were occupied randomly according to the occupation ratios reported in [19]. The k meshes (all Γ-centred) depended on the cell used: 4×4×2 for GeTe, 2×2×2 for GST225. The lattice parameters of the GeTe and GST225 relaxed structures are given in **Table S4** in the supplementary material. They differ from the initial ones by less than 1.6 %. In the case of SLs, we wanted to compare the different models (*Petrov*, *iPetrov*, *Ferro* and *Kooi*) proposed in literature [5]. Note that in these four models, the Ge and Sb atoms occupy separate atomic planes and hence no chemical disorder is present. The models differ by the stacking of the Ge Sb and Te planes. For each model, we used the lattice parameters and atomic positions of the relaxed structures obtained by AIMD simulations in reference [29] and built a hexagonal unit cell containing 9 atoms.

In order to calculate the EXAFS spectra by successive Molecular Dynamics runs, we built super-cells by combining the structurally relaxed cells: (3×3×2, 108 atoms) for GeTe and (3×3×1, 81 atoms) for SLs. In the case of GST225 the super-cell previously used to minimize the energy (3×3×1, 81 atoms) was kept. Molecular Dynamics runs were carried out in the NVT canonical ensemble during a total time of 3 ps. The last 0.9 ps were used to extract the EXAFS spectra that were successively used for generating the theoretical spectrum. For each frame, the spectra, were averaged to obtain the final simulated spectrum. The polarization of the X-ray beam was set parallel to the plane of the Ge absorbers. The temperature was stabilized at 150 K via a Nosé thermostat and monitored along the run.

3. Results

3.1 Experimental EXAFS data

EXAFS spectra of all the deposited $[(GeTe)_2/(Sb_2Te_3)_m]_{24}$ SLs with m varying from 1 to 8 and of the reference GeTe and GST225 films are shown in **Figure 1(a)**. From a qualitative point of view, all the EXAFS spectra of SLs are similar and different from the spectrum of the GeTe film. In particular, large-amplitude oscillations are present in the GeTe spectrum for k values greater than 6 $Å^{-1}$, but not in the SL spectra. Similar EXAFS spectra are expected in GeTe and SLs if the SL contains $(GeTe)_2$ blocks. Instead, the EXAFS spectra of

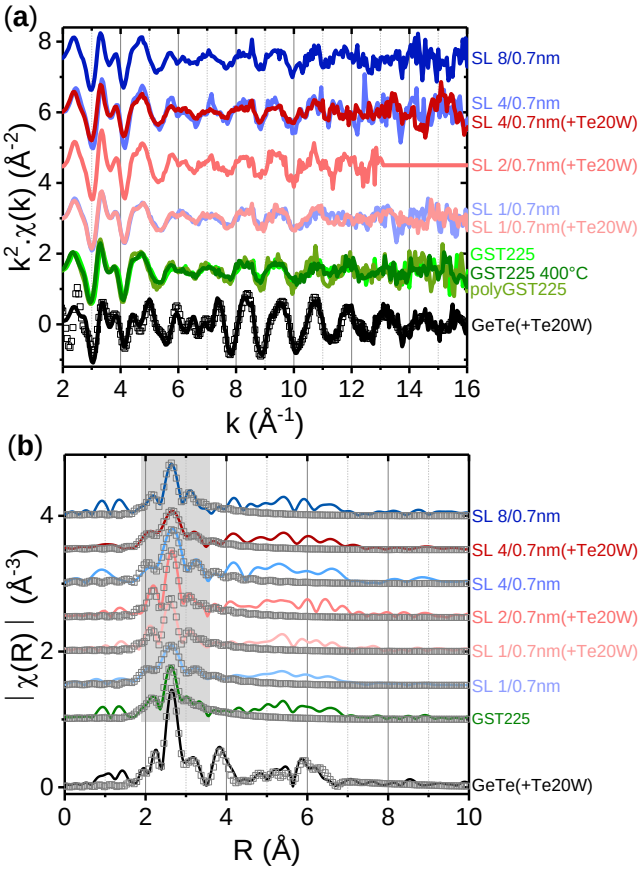

Figure 1. (a) EXAFS spectra acquired at the Ge K-edge on $[(GeTe)_2/(Sb_2Te_3)_m]_{24}$ SLs with m=1, 2, 4 and 8 deposited without Te co-sputtering (labelled SL m/0.7nm) and with Te co-sputtering, with a power of 20 W applied to the Te target, (labelled SL m/0.7nm(+Te20W)), as well as on GeTe and $Ge_2Sb_2Te_5$ (GST225) reference thin films: a GeTe film deposited at 250°C by co-sputtering of GeTe and Te targets (with 20W applied to the Te target) labelled GeTe(+Te20W); three GST225 films deposited by sputtering of a $Ge_2Sb_2Te_5$ target at 250°C (labelled GST225), at 250°C and then annealed at 400°C for 15 min (labelled GST225 400°C) and at room temperature in the amorphous state and then crystallized by annealing at 400°C for 40 min (labelled polyGST225). For the GeTe film the curves with empty symbols is a fit (see text) of the experimental data (solid line).
(b) Fourier transforms of the EXAFS spectra (solid lines) and fits (empty symbols). The R range of the fit (for all samples except for the GeTe(+Te20W) film) is shown by a grey rectangle. In the case of the GeTe(+Te20W) film, a fit based on the rhombohedral crystal structure determined by diffraction [23] has been performed in the R range [1.8-7.2 Å].

the SLs strongly resemble the EXAFS spectra of the GST225 films. Note that the EXAFS spectra of the three GST225 films are similar, although these films were prepared differently and have different crystallite orientations (see **section 2.1**). In the GST225 film deposited at 250°C, the atomic planes are parallel to the substrate, as in SLs. Possible polarization effects, resulting from the XAS measurement configuration, are therefore identical in such an oriented GST225 film and in SLs. The polarization effects ultimately proved to be negligible since the EXAFS spectrum of a GST225 film

containing crystallites with all possible orientations is identical to that of oriented GST225 films. The EXAFS spectra of SLs do not show significant change when the m value changes from 1 to 8. Besides, the spectra of SLs deposited with or without Te co-sputtering are very similar. These striking results show that the local environment of the Ge atoms is not significantly affected by the periodicity or stoichiometry of the SL. The Fourier Transforms (FT) of the EXAFS spectra of **Figure 1(a)** are plotted in **Figure 1(b)**. A qualitative analysis reveals that all FTs have common features in the R range [1.9-3.6 Å], with three maxima at similar R-values. Differences are observed at larger R. In particular, the strong peak present at ~3.9 Å in the GeTe film is absent in the case of SLs and of GST225 films. The FTs of GST225 films and SLs are similar in the full R range, showing maxima at the same R-values. The FT of EXAFS data from [8] measured on a $(GeTe)_{1nm}/(Sb_2Te_3)_{3nm}$ is very similar to that of the stoichiometric and non-stoichiometric $[(GeTe)_2/(Sb_2Te_3)_m]_n$ SLs (with *m*=1, 2, 4 and 8) studied here.

Fits of the FTs have been performed in the R range [1.9-3.6 Å] (**section 2.2.2**) by using a two-shell model. They provide an excellent description of the data, as shown in **Figure 1(b)**. The fit parameters are given in **Table 1**.

Sample	Ge-Te I			Ge-Te II		
	N	R (Å)	σ^2 (Å^2)	N	R (Å)	σ^2 (Å^2)
GeTe	3	2.81(1)	0.0045(8)	3	3.17(2)	0.0073(8)
GST 225	3	2.83(2)	0.0065(9)	3	3.01(2)	0.013(2)
SL 1/0.7 nm	3	2.82(2)	0.012(3)	3	3.06(2)	0.028(8)
SL 4/0.7 nm	3	2.84(2)	0.006(5)	3	3.04(2)	0.02(1)
SL 8/0.7 nm	3	2.85(2)	0.009(3)	3	3.09(2)	0.018(8)
SL 1/0.7 nm + Te20W	3	2.84(2)	0.007(2)	3	3.08(2)	0.017(5)
SL 2/0.7 nm + Te20W	3	2.84(2)	0.007(2)	3	3.01(3)	0.02(1)
SL 4/0.7 nm + Te20W	3	2.83(2)	0.010(5)	3	2.99(3)	0.03(3)

Table 1. Results of fits of EXAFS data. For each shell, the shell radius (R) and the Debye-Waller factor (σ^2) are given. Errors in the last digit are indicated in brackets. The number of Te atoms (N) in each shell has been set at three.

For GeTe, the fit leads to three short and three long Ge-Te distances equal to 2.81(1) Å and 3.17(2) Å, respectively. These values are very close to those calculated from the rhombohedral structure determined by diffraction (given in **Table S3** in the supplementary material). In the rhombohedral GeTe phase, all the Ge atoms have the same environment. The Ge atom is displaced with respect to the centre of the octahedron formed by its Te neighbours and therefore the Ge-Te distances are split into 3 short and 3 long distances. In the case of GeTe, the EXAFS analysis can be successfully performed in a wider R range. The result of a multi-shell calculation based on the average structure determined by diffraction (**section 2.2.2**) is superimposed on the measured data in k and R space in **Figure 1**. The excellent agreement between the calculation and the measured data shows that the local structure around Ge in the GeTe film is that expected from the average structure of the rhombohedral GeTe phase. Note that this agreement was made possible by the absence of a Ge foreign phase in the studied film, as explained in **section 2.1** and in the supplementary material (**Figure S1** and **Table S2**).

For SLs and GST225 films, the fits also lead to a short and a long Ge-Te distance. Remarkably, the Ge-Te distances are almost the same in all these samples, the short distance varying between 2.82 and 2.85 Å and the long one between 2.99 and 3.09 Å respectively (see **Table 1**). Note that this short Ge-Te distance has the same value as in the GeTe film but that the long Ge-Te distance is significantly longer in the GeTe film than in SLs and GST225 film.

Both the short (2.83(2) Å) and the long (3.01(2) Å) Ge-Te distances in GST225 films differ from the values calculated from the average structure determined by diffraction (given in **Table S3** in the supplementary material). In the average structure [19], confirmed by high resolution TEM images [30], there are blocks of nine atomic planes separated by vdW gaps. Inside a block, Te planes alternate with planes occupied by Ge and Sb. There are two crystallographic sites occupied by Ge (and Sb) atoms and hence two Ge/Sb-Te short distances (equal to 2.920 and 2.972 Å) and two long Ge/Sb-Te distances (equal to 3.055 and 3.211 Å). Taking into account the relative occupancy of each site (given in **Table S3** in the supplementary material) the mean Ge-Te short distance is 2.946 Å and the mean Ge-Te long distance is 3.133 Å.

3.2 AIMD simulations of EXAFS spectra

In order to go further and analyse the local order around Ge in a wider R range in GST225 films and in SLs, we performed AIMD simulations of the EXAFS spectra from relaxed structures (see **section 2.3**). We also simulated the EXAFS spectrum of GeTe. The aim was to validate the simulation method since we have shown above that in this case the average structure determined by diffraction and the local structure coincide.

The calculated and measured EXAFS spectra and their FTs are compared in **Figure 2** for GeTe and GST225 films. The agreement is satisfactory for GeTe, whereas in the case of GST225 there is a noticeable shift in the frequency of the oscillations in k space above 6 Å^{-1}. Besides, the amplitude of the oscillations at large k (above ~5 Å^{-1}) is much larger in the simulation than in the measured data. Thus, the simulation cannot account for the local order around Ge in GST25 films. One of the reasons for this discrepancy is that, in the relaxed structure used in the simulation (**Table S5** of the supplementary material), the first Ge-Te distances are different from the measured ones. This point will be discussed in **section 4**.

Figure 3 presents experimental EXAFS spectra and their FTs for two prototypical $[(GeTe)_2/(Sb_2Te_3)_1]_{24}$ SLs, deposited with or without Te co-sputtering, and for the GST225 film, as

well as two AIMD simulations. The *Ferro* simulation is obtained by using the relaxed *Ferro* structure of reference [29] as explained in **section 2.3**. In this structure, there are pure Ge and Sb planes within blocks of nine Te/Ge/Te/Ge/Te/Sb/Te/Sb/Te planes separated by vdW gaps. The calculated EXAFS oscillations are in phase with the experimental ones. This agreement indicates that the distances of the relaxed structure are correct, as can also be seen when comparing the experimental and calculated TFs. However, the amplitude of the oscillations of the calculated spectrum is too large, compared to those measured. The AIMD simulations of

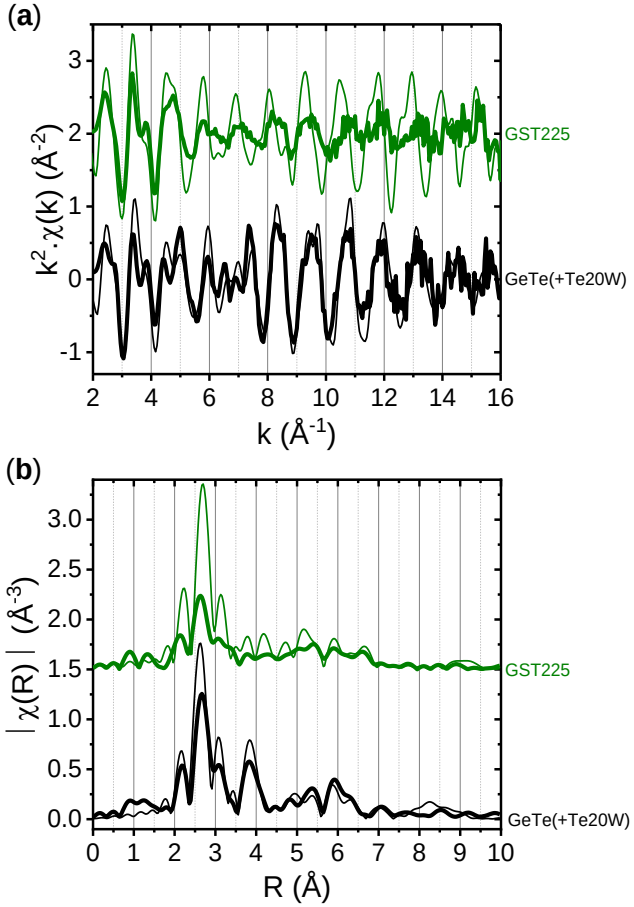

Figure 2. (a) EXAFS spectra and ***(b)*** corresponding Fourier transforms measured on reference GST225 and GeTe films (thick solid lines). The AIMD simulations of the EXAFS data, calculated from the relaxed average crystal structure determined by diffraction, are also plotted in thin lines (see text).

the EXAFS spectra from relaxed structures for the other models proposed for the SLs (*Ferro*, *Petrov*, *iPetrov* and *Kooi* structures shown in **Figure S8**) are shown in **Figure S9** of the supplementary material. Again, the amplitude of the oscillations at large k (above ~5 $Å^{-1}$) is much larger in the simulation than in the measured data. Therefore, none of these models can account for the measured EXAFS spectra in SLs. As shown in the discussion below, one reason is that all these models assume pure Ge and Sb atomic planes.

4. Discussion

To summarize, we have shown that the local order around Ge atoms is the same for all studied stoichiometric and non-stoichiometric $[(GeTe)_2/(Sb_2Te_3)_m]_n$ SLs (with m=1, 2, 4 and 8). This conclusion is in agreement with the results reported in reference [14] showing that the X-ray absorption near edge structure does not vary with the thickness of the deposited Sb_2Te_3 layer. Moreover, the local order strongly resembles that of crystalline GST225 thin film whatever the m value. In particular, the short and long Ge-Te distances (2.82-2.85 Å and 2.99-3.09 Å, respectively) are the same in all SLs and in the GST225 thin films. They result from Peierls distortions, which are also at origin of the short and long Ge-Te distances in GeTe. However, in the latter case the Ge-Te distances are in excellent agreement with those calculated from the crystallographic structure determined by diffraction [23]. This is due to the absence of disorder in the rhombohedral GeTe phase. The discrepancy between the actual Ge-Te distances and those calculated from the average structure of the rhombohedral GST225 phase determined by X-ray diffraction [19] can be explained by the mixed occupancy of the cation planes by Ge and Sb. In presence of a chemical disorder, the diffraction determines only the average position of the Ge and Sb atoms and not their actual positions. Thus, in that case, the Ge-Te and Sb-Te distances deduced from diffraction are identical, whereas in reality they certainly differ. This is the case in in the metastable cubic phase of GST225. EXAFS at the Ge and Sb K-edges have shown that the short Sb-Te distance is equal to 2.91(1) Å, and the short Ge-Te distance is equal to 2.83(1) Å [31]. It is striking that the short Ge-Te distance measured in rhombohedral GST225 (2.83(2) Å) in the present work is equal to the short Ge-Te distance in the metastable cubic phase of GST225 [31]. The MD simulated GSST225 rhombohedral structure of the present study uses as a starting point the crystallographic structure determined from diffraction [19]. The fact that this simulation could not account for the measured Ge-Te distances results from a too short relaxation time upon MD-simulation, which did not allow the Ge and Sb atoms to reach their final equilibrium position.

Besides, one observes that for SLs and GST225 films the Debye-Waller factors (σ^2) for the long Ge-Te distance are systematically higher (by at least a factor 2) than for the short Ge-Te distance. This observation also applies to the Ge-Te film but in the latter case the σ^2 values are smaller and the ratio between the σ^2 values for short and long distance is smaller. One can reasonably ascribe this effect to a static disorder present in SLs and GST225 compared with GeTe where the σ^2 value mainly results from thermal vibrations. The issue of the structure of GeTe/SbTe SLs has been addressed in TEM studies that have evidenced that Ge atoms inter-diffuse into the adjacent Sb_2Te_3 layers creating locally $Ge_2Sb_2Te_5$ blocks and other Ge-Sb-Te (GST) blocks containing either 7, 11 … atomic planes depending on the m value [7-11, 13]. Hence, different Ge environments exist due to the different nature the

GST blocks separated by the vdW gaps. In each type of GST block, the occupation of the cation plane by Ge and Sb depends on the plane position with respect to the vdW gap as shown in [12, 30].

The fact that the MD simulation of the *Ferro* relaxed model provides EXAFS oscillations in phase with the experimental ones indicates that the Ge-Te distances of this relaxed structure are correct, as shown in **Table S6** in the supplementary material. Nevertheless, if this *Ferro* model has the correct Ge-Te distances, it does not include the chemical disorder. In order to investigate the role of chemical disorder, we artificially introduced chemical disorder in the *Ferro* model. We randomly exchanged 1/3 of the Ge with Sb atoms and let the new structure relax via MD (see the snapshots of such *Ferro-intermix* model in **Figure S7** of the supplementary material). As shown in **Figure 3**, the introduction of disorder by randomly mixing 1/3 of the Ge/Sb sites does not significantly affect the Ge-Te distances (**Table S6**) but leads to a damping of the oscillations at large k compared to the MD-*Ferro* model. Hence, the MD-*Ferro-intermix* simulation is closer to the experiment. In particular the overall shape of the χ(k) is better reproduced in the region 5.5-8 Å^{-1} and the intermixing damps the peak at 4 Å in the FT that is present in the ideal *Ferro* model but absent in the experimental data of the SL. This attempt proves that chemical disorder is present in all SLs as in GST225 thin film.

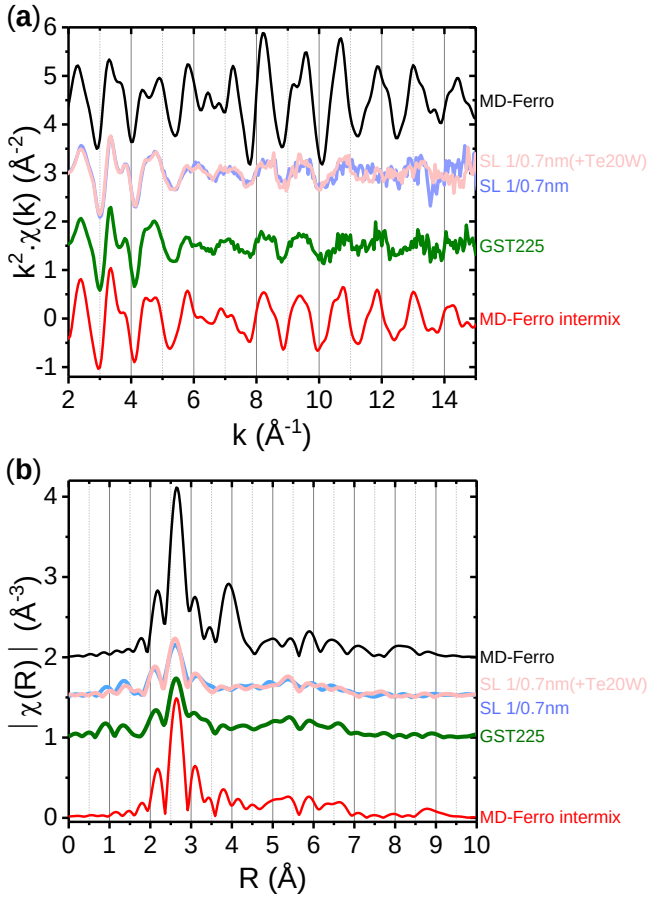

Figure 3. (a) EXAFS spectra and ***(b)*** corresponding Fourier transforms measured on $[(GeTe)_2/(Sb_2Te_3)_1]_{24}$ SLs, with or without Te co-sputtering (labelled SL 1/0.7nm(+Te20W) and SL 1/0.7nm, respectively) and on the $Ge_2Sb_2Te_5$ (GST225) reference film represented by thick solid lines. AIMD simulations (see text) of the EXAFS data for the *Ferro* structural model, either with pure Ge and Sb atomic planes (labelled MD-*Ferro*, thin black line), or with mixed Ge/Sb occupation of the atomic planes (labelled MD-*Ferro intermix*, thin red line).

5. Conclusion

In this work we have analysed the local structure of $[(GeTe)_2/(Sb_2Te_3)_4]_{24}$ super-lattices (SLs) using XAS at the Ge-K edge. From a qualitative analysis, the SLs appear to possess a structure very similar to that of GST225 films. This is confirmed by the quantitative analysis of the first coordination shells. The comparison between experimental data and *ab initio* simulated EXAFS spectra shows that chemical disorder is required in order to reproduce the EXAFS spectra. Then, we can conclude that Ge/Sb intermixing resulting from inter-diffusion of the GeTe and Sb_2Te_3 layers within SLs, that had been mostly evidenced by TEM studies, is inherent to SLs and not induced by TEM foil preparation method nor by interaction with the electron beam. Moreover, from the present study, one can conclude that the short Ge-Te distance is the same in GeTe and GST225 films as well as in SLs. The main difference between these systems is the impact of disorder in GST225 and SLs, as seen from the Debye-Waller factors. To conclude, intermixing is undoubtedly present in $[(GeTe)_2/(Sb_2Te_3)_m]_n$ SLs and deserve further experimental studies in both thin films and devices in order to be able to unambiguously unveil one day the origin of electrical switching in iPCM devices. Such an understanding is mandatory to go further in the development of iPCM technology as well as permitting the latter to emerge in the near future on the non-volatile memory market.

Acknowledgments

This work has been partially supported by the European 621217 PANACHE and 783176 WAKeMeUP Projects. M. Bernard and L. Fellouh are gratefully acknowledged for their support on the deposition tool and in-line characterization facilities. XAS measurements with synchrotron radiation were performed at the BM08/LISA beamline (former GILDA beamline) of the European synchrotron (ESRF) thanks to beamtimes under experience numbers MA-2719 and MA-3172. LISA is a project funded by the Consiglio Nazionale delle Richerche (project DFM.AD006.072). JYR acknowledges support from the FRS-FNRS.

References

[1] Noé P, Vallée C, Hippert F, Fillot F and Raty J 2017 Semiconductor Science and Technology 33 013002

[2] M. Wuttig, V. L. Deringer, X. Gonze, C. Bichara, J.-Y. Raty, 2018 Adv. Mater. 30 1803777.
[3] J.-Y. Raty, M. Schumacher, P. Golub, V. L. Deringer, C. Gatti, M. Wuttig, A 2019 Adv. Mater. 31 1806280.
[4] Simpson R E, Fons P, Kolobov A V, Fukaya T, Krbal M, Yagi T and Tominaga J 2011 Nature Nanotechnology 6 501–505
[5] Tominaga J, Kolobov A V, Fons P, Nakano T and Murakami S 2014 Advanced Materials Interfaces 1 1300027
[6] Tominaga, J, 2019 Physica Status Solidi (RRL) – Rapid Research Letters 13 1800539.
[7] Momand J, Wang R, Boschker J E, Verheijen M A, Calarco R and Kooi B J 2015 Interface formation of two- and three-dimensionally bonded materials in the case of GeTe–Sb2Te3 superlattices *Nanoscale* **7** 19136–43
[8] Casarin B, Caretta A, Momand J, Kooi B, Verheijen M, Bragaglia V, Calarco R, Chukalina M, Yu X, Robertson J, Lange F R L, Wuttig M, Redaelli A, Varesi E, Parmigiani F and Malvestuto M 2016 Scientific Reports 6 22353
[9] Lotnyk A, Ulrich I H and Rauschenbach B 2018 Nano Research 11 1676
[10] Momand J, Lange F R L, Wang R, Boschker J E, Verheijen M, Calarco R, Wuttig M and Kooi B J 2016 Journal of Materials Research 31 3115–3124
[11] Kowalczyk P, Hippert F, Bernier N, Mocuta C, Sabbione C, Batista-Pessoa W and Noé P 2018 Small 14 1704514
[12] Lotnyk A, Ross U, Dankwort T, Hilmi I, Kienle L and Rauschenbach B 2017 Acta Materialia 141 92–96
[13] Kooi B J and Momand J 2019 Physica Status Solidi (RRL) – Rapid Research Letters 13 1800562
[14] Saito Y, Fons P, Mitrofanov K V, Makino K, Tominaga J, Robertson J and Kolobov A V 2019 *Pure and Applied Chemistry* **91** 1777–86.
[15] Kalikka J, Zhou X, Dilcher E, Wall S, Li J and Simpson R E 2016 Nature Communications 7 11983
[16] Shelimova L E, Karpinskii O G, Kretova M a., Kosyakov V I, Shestakov V a., Zemskov V S and Kuznetsov F A. 2000 Inorganic Materials 36 768–775
[17] Anderson T L and Krause H B 1974 Acta Cryst. B 30 1307‑10
[18] Hippert F, Kowalczyk P, Bernier N, Sabbione C, Zucchi X, Térébénec D, Mocuta C and Noé P 2020 J. Phys. D: Appl. Phys. 53 154003
[19] Urban P, Schneider M, Erra L, Welzmiller S, Fahrnbauer F and Oeckler O 2013 CrystEngComm 15 4823–4829
[20] Matsunaga T, Morita H, Kojima R, Yamada N, Kifune K, Kubota Y, Tabata Y, Kim J-J, Kobata M, Ikenaga E and Kobayashi K 2008 J. of Appl. Phys. 103 093511
[21] Schlieper A, Feutelais Y, Fries S G, Legendre B and Blachnik R 1999 Calphad 23 1–18
[22] Noé P and Hippert F 2018 Structure and Properties of Chalcogenide Materials for PCM Phase Change Memory (Springer, Cham) pp 125–179
[23] Chattopadhyay T, Boucherle J X and von Schnering H G 1987 J. Phys. C: Solid State Phys. 20 1431-1440
[24] d'Acapito F, Trapananti A, Torrengo S and Mobilio S 2014 Notiziario Neutroni e Luce di Sincrotrone 19 14–23
[25] Maurizio C, Rovezzi M, Bardelli F, Pais H G and D'Acapito F 2009 Review of Scientific Instruments 80 063904
[26] Ravel B and Newville M 2005 J. Synchrotron Radiat. 12 537–541
[27] Kresse G and Furthmüller J 1996 Phys. Rev. B 54 11169
[28] Csonka G I, Perdew J, Ruzsinszky A, Philipsen P H T, Lebègue S, Paier J, Vydrov O and Ángyán J 2009 Phys. Rev. B 79(15) 155107
[29] Ibarra-Hernández W and Raty J-Y 2018 Phys. Rev. B 97 245205
[30] Lotnyk A, Ross U, Bernütz S, Thelander E and Rauschenbach B 2016 Sci Rep 6 26724
[31] Kolobov A V, Fons P, Frenkel A I, Ankudinov A L, Tominaga J and Uruga T 2004 Nature Mater 3 703–8